

Hadronic Production of the Doubly Charmed Baryon Ξ_{cc} with Intrinsic Charm

Chao-Hsi Chang^{1,2}, Jian-Ping Ma², Cong-Feng Qiao³ and Xing-Gang Wu^{2,4}

¹*CCAST (World Laboratory), P.O.Box 8730, Beijing 100080, P.R. China*

²*Institute of Theoretical Physics, Chinese Academy of Sciences,*

P.O.Box 2735, Beijing 100080, P.R. China

³*Department of Physics, Graduate University,*

Chinese Academy of Sciences, Beijing 100049, P.R. China

⁴*Department of Physics, Chongqing University, Chongqing 400044, P.R. China*

Abstract

The effects of the intrinsic charm on the hadronic production of Ξ_{cc} are studied. By taking reasonable intrinsic charm component into account, the change of the theoretical prediction on the production of Ξ_{cc} for LHC and Tevatron is small, but in contrast it may enhance significantly for SELEX. The reason is that the collision energy at LHC and Tevatron is so large that the gluon-gluon fusion sub-process, which is irrelevant to intrinsic charm, becomes dominant. But the situation for SELEX is quite different. Our numerical results for SELEX show that by considering all the contributions from various sub-processes, the predicted cross-section may be enhanced by a factor so big as 10^2 due to a modulating intrinsic charm being taken into account. Therefore, the hadronic production of Ξ_{cc} at SELEX may be sensitive enough in observing the intrinsic charm inside the incident hadrons.

PACS numbers: 12.38.Bx, 12.39.Jh, 13.87.Ce, 14.20.Lq

I. INTRODUCTION

SELEX Collaboration [1, 2] has reported the observation of the doubly charmed baryon Ξ_{cc}^+ , which contains two charm quarks. According to their measurement, the decay width and production rate, nevertheless, are much larger than expected [3, 4, 5, 6, 7]. The theoretical predictions based on gluon-gluon fusions in [3, 4, 5, 6, 7] are much smaller than the measured cross-section by order of about 10^3 . Several possible mechanisms for the hadronic production of Ξ_{cc}^+ are proposed, the discrepancy between experimental data and theoretical predications decreases but it is still there [8] and it is at order of about 10^2 . Since the baryon Ξ_{cc} , either Ξ_{cc}^+ or Ξ_{cc}^{++} , is doubly charmed, here we will highlight the intrinsic charm in the colliding hadrons through studying the hadronic production of Ξ_{cc} at different situations (e.g. at LHC, Tevatron and SELEX).

In the hadronic production, the Ξ_{cc} is produced through scattering or annihilating or fusion of two initial partons inside the incident hadrons. Although the common belief is that the gluon-gluon fusion mechanism is important and even dominant in high energy hadron collision, the other mechanisms may be still substantial sometimes. For the other mechanisms, besides the light partons, it is also possible to find certain importance of heavy quarks inside the initial hadrons, whose possibilities are described by the corresponding heavy quark distribution function. The lightest heavy-flavored charm-quark, being as a parton, can be generated in different ways inside the incident hadrons. The heavy quark (charm or bottom) component in parton distribution functions (PDFs) can be perturbatively generated by gluon splitting, and hence is named as the ‘extrinsic’ component according to Ref.[8]. It can also be generated non-perturbatively and appears at or even below the energy scale of heavy quark threshold. This component is normally called as ‘intrinsic’ one according to Refs.[9, 10, 11, 12, 13]. The extrinsic charm contribution to the Ξ_{cc} hadronic production has been studied in Ref.[8] within the general-mass variable-flavor-number (GM-VFN) scheme [14, 15, 16]. It is shown that the extrinsic charm contribution is substantially large at the energy range of SELEX experiment [8], i.e., the extrinsic charm can raise the total hadronic cross-section of Ξ_{cc} by almost an order of magnitude in comparison with that only from the gluon-gluon fusion mechanism. It is also interesting to investigate how much the intrinsic charm may contribute in the hadronic production, specially to see where and to what ‘degree’ the intrinsic charm component in concerned hadron can be determined. In

fact, the existence of the intrinsic heavy flavor components in a proton has been supported by some experiments and theoretical predictions. For instance, the intrinsic heavy flavors are adopted to study the diffractive Higgs production in Ref.[17], where the authors have pointed out that a clear experimental signal for Higgs can be observed due to the existence of intrinsic heavy flavor components inside the nucleon. Bearing the problem of the intrinsic charm inside a nucleon in mind, we will examine the intrinsic charm effects on the Ξ_{cc} hadronic production at different experiment situations, i.e. at LHC, Tevatron and SELEX, and see which is the best place to perform the measurements on the intrinsic charms¹.

In fact, the intrinsic charm quark content of proton is still not well determined. In the latest versions of PDF, like CTEQ [18], GRV [19] and MRST [20], the heavy quark components arise only perturbatively through gluon splitting, which means they have the extrinsic nature. Although these PDFs are determined through the global fitting, it can not rule out the intrinsic component with certain possibility because the data for fitting does not include those experiment results which are sensitive to the intrinsic heavy quark reactions [9]. At present, the probability magnitude of the intrinsic charm within nucleon has not been well fixed yet. Nevertheless, we know it can not be large in order to comply with the global fitting result. Upper-bounds for the probability of the intrinsic charm A_{in} inside nucleon, i.e., the first moment of the intrinsic charm quark PDF at a lower energy scale (e.g. $\mu^2 \sim m_c^2$) is available: according to Refs.[9, 10, 11, 12], A_{in} can not be much larger than 1%; and another one, $(0.86 \pm 0.60)\%$, is obtained by analysis of F_2^c data in deep inelastic muon scattering on iron [21, 22]. The intrinsic charm PDF can only be studied with some nonperturbative methods with models. Recently, the operator product expansion method shows that the probability for Fock states in light hadron to have an extra heavy quark pair of mass M_Q decreases as Λ_{QCD}^2/M_Q^2 in non-Abelian gauge theory [23]. In the present work for definiteness, we will take the BHPS model [13] as a typical example for the intrinsic charm to study the Ξ_{cc} hadronic production.

The paper is organized as follows. In Sec.II, we outline the techniques for calculating the Ξ_{cc} hadronic production under the GM-VFN scheme. Specially, we will show how we obtain the requested PDF of charm quark at the higher energy scale through CTEQ6HQ

¹ Since there are some puzzles in hadronic production of J/ψ still, thus we think that any determination on the intrinsic charm components of the PDFs of the incident hadrons cannot be decisive.

plus the intrinsic charm component obtained by solving DGLAP equation with proper initial boundary condition at low energy scale. In Sec.III, we present the numerical results for the Ξ_{cc} hadronic production. The final section is reserved for discussions and summary.

II. CALCULATION TECHNIQUES

With QCD factorization and the GM-VFN scheme, the differential cross-section for the inclusive hadronic production of $H_1 + H_2 \rightarrow \Xi_{cc} + X$ can be written as the convolution

$$\begin{aligned} \sigma &= f_{H_1}^g(x_1, \mu) f_{H_2}^g(x_2, \mu) \otimes \hat{\sigma}_{gg \rightarrow \Xi_{cc}}(x_1, x_2, \mu) \\ &+ \left\{ \sum_{i,j=1,2; i \neq j} f_{H_i}^g(x_1, \mu) \left[f_{H_j}^c(x_2, \mu) - f_{H_j}^c(x_2, \mu)_{SUB} \right] \otimes \hat{\sigma}_{gc \rightarrow \Xi_{cc}}(x_1, x_2, \mu) \right\} \\ &+ \left\{ \sum_{i,j=1,2; i \neq j} \left[\left(f_{H_i}^c(x_1, \mu) - f_{H_i}^c(x_1, \mu)_{SUB} \right) \cdot \left(f_{H_j}^c(x_2, \mu) - f_{H_j}^c(x_2, \mu)_{SUB} \right) \right] \right. \\ &\quad \left. \otimes \hat{\sigma}_{cc \rightarrow \Xi_{cc}}(x_1, x_2, \mu) \right\} + \dots, \end{aligned} \quad (1)$$

where μ is the renormalization (factorization) scale, the ellipsis stands for contributions from higher order in α_s and from light quarks initiate processes. The later are much smaller than those given explicitly in Eq.(1). $f_H^a(a = g, c)$ is the PDF of the corresponding parton a and $f_H^c(x, \mu)_{SUB}$ is defined in the GM-VFN scheme as

$$f_H^c(x, \mu)_{SUB} \equiv f_H^g(x, \mu) \otimes f_g^c(x, \mu) = \int_x^1 \frac{dy}{y} f_g^c(y, \mu) f_H^g\left(\frac{x}{y}, \mu\right) \quad (2)$$

with

$$f_g^c(x, \mu) = \frac{\alpha_s(\mu)}{2\pi} \ln \frac{\mu^2}{m_c^2} P_{g \rightarrow q}(x) = \frac{\alpha_s(\mu)}{2\pi} \ln \frac{\mu^2}{m_c^2} \cdot \frac{1}{2} (1 - 2x + 2x^2). \quad (3)$$

To be realistic we will consider only the Ξ_{cc} with nonzero transverse momentum p_t . Therefore, the partonic cross-sections in Eq.(1) represent various parton processes at leading order in α_s . The $\hat{\sigma}_{gg \rightarrow \Xi_{cc}}$ stands for $g + g \rightarrow \Xi_{cc} + \bar{c} + \bar{c}$, $\hat{\sigma}_{gc \rightarrow \Xi_{cc}}$ stands for $g + c \rightarrow \Xi_{cc} + \bar{c}$ and $\hat{\sigma}_{cc \rightarrow \Xi_{cc}}$ for $c + c \rightarrow \Xi_{cc} + g$. These partonic cross-sections can be further factorized if we take charm quark as heavy quark. In this case, charm quarks inside the rest Ξ_{cc} move with a small velocity v . One can systematically expand the partonic cross-sections in Eq.(1) in v by using nonrelativistic QCD (NRQCD) [24] to separate perturbative and nonperturbative effects. In this framework the partonic cross-section can be expressed as [25]:

$$\hat{\sigma}_{ab \rightarrow \Xi_{cc}} = H(ab \rightarrow (cc)[^3S_1]_{\mathbf{3}}) \cdot h_3 + H(ab \rightarrow (cc)[^1S_0]_{\mathbf{6}}) \cdot h_1 + \dots, \quad (4)$$

where the ellipsis stands for the terms in higher orders of v . $H(ab \rightarrow (cc)[^3S_1]_{\bar{\mathbf{3}}})$ or $H(ab \rightarrow (cc)[^1S_0]_{\mathbf{6}})$ is the perturbative coefficient for producing a cc pair in configuration of 3S_1 and color $\bar{\mathbf{3}}$, or 1S_0 and color $\mathbf{6}$ respectively [8]. The parameters h_3 and h_1 characterize the transitions of a $(cc)[^3S_1]_{\bar{\mathbf{3}}}$ pair and a $(cc)[^1S_0]_{\mathbf{6}}$ pair into the produced Ξ_{cc} , respectively. They are nonperturbative in nature and are just the relevant matrix elements in NRQCD framework (see Eq.(4)). It has been pointed out in [25] that these two parameters are at the same order of v , so for convenience and to decrease the ‘freedom’ of the prediction, hereafter we assume h_1 is equal to h_3 .

Now we turn to the part on how to deal with the additional contributions from the intrinsic charm components to the charm PDF. It is generally expected that the intrinsic heavy quark component in PDFs is proportional to Λ_{QCD}^2/M_Q^2 with M_Q being the mass of the heavy quark [23]. Therefore, in general the heavy quark components are small, so we will treat the intrinsic charm component as a small perturbation to the current determined PDFs. We will also take the leading order DGLAP equation for its and the relevant gluon component evolution. Hence, at leading order the introduction of the intrinsic charm component will not affect the PDFs of light quarks, but will affect the gluon’s PDF. Under the above approximation the charm- and gluon- PDFs can be written as:

$$f_H^c(x, \mu) = f_H^{c, ex}(x, \mu) + f_H^{c, in}(x, \mu), \quad (5)$$

$$f_H^g(x, \mu) = f_H^{g, ex}(x, \mu) + f_H^{g, in}(x, \mu). \quad (6)$$

In the above equations, $f_H^{c, ex}(x, \mu)$ is the extrinsic charm component that is already determined by the global fitting of several groups. $f_H^{c, in}(x, \mu)$ stands for the intrinsic charm component. The intrinsic charm component will also induce a small change to the currently determined gluon PDF, which is denoted as $f_H^{g, in}(x, \mu)$. Hence, the gluon PDF is the sum of the change $f_H^{g, in}(x, \mu)$ and the currently determined gluon PDF $f_H^{g, ex}(x, \mu)$.

The intrinsic charm component can not be calculated with pQCD. It can be introduced only with nonperturbative methods at some lower energy scale. Several models have been constructed for $f_P^{c, in}(x, \mu)_{\mu=2m_c}$ in a proton [9, 26]. The function $f_P^{c, in}(x, \mu)_{\mu=2m_c}$ from various models constructed in Ref.[9] is close to that of the BHPS model [13] in shape, so we will take BHPS model as a typical one in our numerical studies. In this model the intrinsic charm component at $\mu = 2m_c$ is parameterized as:

$$f_P^{c, in}(x, 2m_c) = f_P^{\bar{c}, in}(x, 2m_c) = 6\xi \left[6x(1+x) \ln x + (1-x)(1+10x+x^2) \right] x^2, \quad (7)$$

where P stands for the proton, the parameter ξ is determined by the first momentum of the distribution, i.e., the probability to find a charm quark in total:

$$A_{in} \equiv \int_0^1 f_P^{c, in}(x, 2m_c) dx = \xi \times 1\% .$$

When $\xi = 1$, it means that the probability for finding c/\bar{c} -component in proton at the fixed low-energy scale $2m_c$ is 1% as suggested in [12, 13]. In the following, we will take a broader range $\xi \in [0.1, 1]$ to do our discussions ². The charm content in an anti-proton is the same as that in a proton. Since we will only deal proton-proton or proton-anti-proton scattering we will suppress the subscript H for PDFs and introduce shorthand notations for those in Eq.(4):

$$f_H^{c, in} = f_c^{in}, \quad f_H^{g, in} = f_g^{in}, \quad f_H^{c, ex} = f_c^0, \quad f_H^{g, ex} = f_g^0, \quad f_H^c = f_c, \quad f_H^g = f_g, \quad (8)$$

where H stands for a proton or anti-proton.

With the intrinsic component fixed at the initial scale $2m_c$ we can obtain the distributions at any higher scale μ by employing the DGLAP equation. Taking the leading order equation, we use the approximate method of Ref.[27] to solve the DGLAP equations for $f_c^{in}(x, \mu)$ and $f_g^{in}(x, \mu)$. The solutions are:

$$\begin{aligned} f_c^{in}(x, \mu) &= \int_x^1 \frac{dy}{y} \left\{ f_c^{in}(x/y, 2m_c) \frac{[-\ln(y)]^{a\kappa-1}}{\Gamma(a\kappa)} \right\} + \\ &\quad \kappa \int_x^1 \frac{dy}{y} \int_y^1 \frac{dz}{z} \left\{ f_c^{in}(y/z, 2m_c) \frac{[-\ln(z)]^{a\kappa-1}}{\Gamma(a\kappa)} P_{\Delta c}(x/y) \right\} + \mathcal{O}(\kappa^2) \\ f_g^{in}(x, \mu) &= \frac{2\kappa}{a_g - a_c} \int_x^1 \frac{dy}{y} \int_{a_c}^{a_g} da \int_y^1 \frac{dz}{z} \left\{ f_c^{in}(z, 2m_c) \frac{[-\ln(z)]^{a\kappa-1}}{\Gamma(a\kappa)} P_{c \rightarrow gc}(x/y) \right\} + \mathcal{O}(\kappa^2) \end{aligned}$$

with

$$\begin{aligned} a_g &= 6, \quad a_c = \frac{8}{3}, \quad \kappa = \frac{2}{\beta_0} \ln \left(\frac{\alpha_s(2m_c)}{\alpha_s(\mu)} \right), \quad \beta_0 = 11 - 2n_f/3, \\ P_{\Delta c}(x) &= \frac{4}{3} \left[\frac{1+x^2}{1-x} + \frac{2}{\ln x} + \left(\frac{3}{2} - 2\gamma_E \right) \delta(1-x) \right], \\ P_{c \rightarrow gc} &= \frac{4}{3} \left[\frac{1+(1-x)^2}{x} \right]. \end{aligned} \quad (10)$$

where n_f is the number of the flavor, and is taken to be 4. It should be noted that $P_{\Delta c}$ is not exactly the splitting function $P_{c \rightarrow gc}$ [27]. With the above equations we can obtain PDF's

² A quite smaller value of $A_{in} \sim 10^{-5}$ has been suggested in Ref.[26], since it is model dependent, we will not take such a small value to do our calculation.

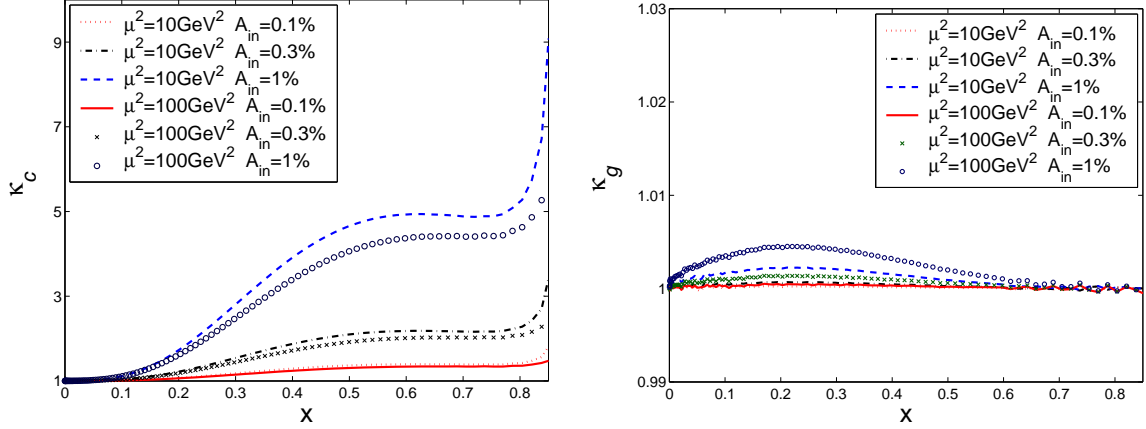


FIG. 1: The ratio $\kappa_c = f_c(x, \mu)/f_c^0(x, \mu)$ (left) and the ratio $\kappa_g = f_g(x, \mu)/f_g^0(x, \mu)$ (right). Two energy scales and three typical normalization for the intrinsic charm, $A_{in} = 0.1\%$, 0.3% and 1% , are taken respectively.

at any scale. To make the employed approximation valid, it has been suggested in Ref.[27] that κ given in Eq.(9,10) should be smaller than 0.3. We have checked this in our case with $\mu = M_t \equiv \sqrt{m_{\Xi_{cc}}^2 + p_t^2}$. For all ranges of μ used here κ is smaller than 0.2. Since we include the intrinsic charm in PDF, the PDF of light quarks and gluons will also be changed in order to satisfy the momentum sum rule. This change can be expected to be at order of κ^2 and leads to a violation of the momentum sum rule at 1% level with $A_{in} = 1\%$. We will simply neglect this change since the change is small.

To see how the intrinsic charm component modifies the PDFs, the ratios $\kappa_c = f_c(x, \mu)/f_c^0(x, \mu)$ and $\kappa_g = f_g(x, \mu)/f_g^0(x, \mu)$ are plotted in Fig.1 at the energy scales of $\mu^2 = 10\text{GeV}^2$ and $\mu^2 = 100\text{GeV}^2$ with $A_{in} = 0.1\%$, 0.3% and 1% . The distributions with the same parameters are plotted in Fig.2. From Fig.1 one can see that the intrinsic charm component changes the charm PDF significantly and κ_c increases as x increases. When $x > 0.8$ the change of the charm PDF after including the intrinsic charm component is too large to warrant the used approximations. Fortunately, the x which leads to the dominant contributions to differential cross section falls in the intermediate region. Our numerical study also shows that the PDFs in the region of $x \geq 0.8$ only give negligible contributions to differential cross-sections. From Fig.1 and Fig.2 we can see that the change of the gluon PDF by including the intrinsic charm component is indistinctive as expected.

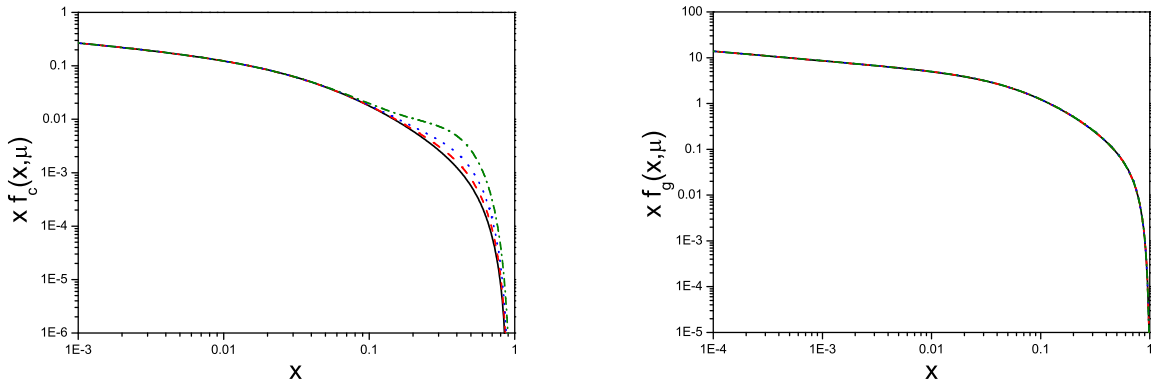


FIG. 2: The charm PDF (left) and gluon PDF (right) at $\mu^2 = 10 \text{ GeV}^2$. The solid line is for $x f_c^0(x, \mu)$ or $x f_g^0(x, \mu)$. The dashed line, the dotted line and the dash-dot line are for $x f_c(x, \mu)$ or $x f_g(x, \mu)$ with $A_{in} = 0.1\%$, 0.3% and 1% , respectively.

III. NUMERICAL RESULTS OF DIFFERENTIAL CROSS-SECTIONS

In order to make numerical estimations on the differential cross-sections we need to know the parameters h_1 and h_3 . Unfortunately, they are unknown. For simplicity, we will take $h_1 = h_3$ as claimed in above. If one uses a nonrelativistic wave function $\Psi_{(cc)}$ for the 3S_1 cc pair in the color $\bar{\mathbf{3}}$ state, then we have $h_3 = |\Psi_{(cc)}(0)|^2$ [25]. We take $h_3 = |\Psi_{(cc)}(0)|^2 = 0.039 \text{ GeV}^3$ as in [5]. The uncertainties from the values of h_1 and h_3 can be easily obtained, since they are overall factors for the processes. For masses we take $m_{\Xi_{cc}} = 3.50 \text{ GeV}$ and $m_c^{eff} = 1.75 \text{ GeV}$. The energy scale μ is fixed to be the transverse mass of Ξ_{cc} , i.e. $\mu = M_t \equiv \sqrt{m_{\Xi_{cc}}^2 + p_t^2}$, where p_t is the transverse momentum of the baryon. In dealing with the running coupling α_s we take $n_f = 4$ and $\Lambda_{QCD}^{(n_f=4)} = 0.215 \text{ GeV}$. For all the numerical evaluations in the following we make use of the CTEQ6HQ version of PDFs. The analytical and numerical results are obtained by using well-established codes of BCVEGPY [28] and FDC [29]. Furthermore, one can conveniently use the newly developed generator GENXICC to study the hadronic production of Ξ_{cc} [30].

TABLE I: The contribution of σ_{ab} from different sub-processes initialized by the partons ab to the total cross section (in pb) for the Ξ_{cc} hadronic production at SELEX with the cut of $p_t > 0.2$ GeV.

-	CTEQ6HQ($A_{in} = 0$)			$A_{in} = 1\%$		
-	σ_{gg}	σ_{cc}	σ_{gc}	σ_{gg}	σ_{cc}	σ_{gc}
$(cc)_{\mathbf{\bar{3}}}[^3S_1]$	4.03	1.02×10^{-3}	102.	4.06	1.25×10^{-2}	372.
$(cc)_{\mathbf{6}}[^1S_0]$	0.754	4.15×10^{-5}	11.3	0.758	5.01×10^{-4}	40.9

TABLE II: The contribution rates of the sub-process $gc \rightarrow \Xi_{cc}$ in the different x region in the charm quark PDFs with $A_{in} = 1\%$ and $p_t > 0.2$ GeV.

$0.0 \leq x_c \leq 0.2$	$0.2 \leq x_c \leq 0.4$	$0.4 \leq x_c \leq 0.6$	$0.6 \leq x_c \leq 0.8$	$0.8 \leq x_c \leq 1.0$
25%	50%	22%	3%	~ 0

A. Hadronic production of Ξ_{cc} at SELEX

The cross-sections receive contributions from different sub-processes. To see how these sub-processes contribute to Ξ_{cc} production cross-sections we give our numerical results of different sub-processes in TABLE.I, where we indicate explicitly the initial parton states and the final cc pair states. From TABLE.I it is obvious that the intrinsic charm has the most significant impact on the contribution from the sub-process $gc \rightarrow \Xi_{cc}$. Also to note that this sub-process gives the dominant contribution to the total cross-section with $A_{in} = 0$ or $A_{in} = 1\%$. By taking $A_{in} = 1\%$ the contribution is roughly four times larger than that without intrinsic charm. Taking the $g + c$ sub-process as an explicit example, we present how the different regions of x in the charm quark PDFs contribute to the sub-process in TABLE.II. From TABLE.II. one can see that the region $x > 0.6$ gives tiny contribution and the main contribution comes from $0.2 < x < 0.4$. We also note that in TABLE.I. the contribution from the quark pair $c\bar{c}$ in the configuration $(c\bar{c})_{\mathbf{6}}[^1S_0]$ are generally smaller by a factor of about 10^{-1} than that in the configuration $(c\bar{c})_{\mathbf{\bar{3}}}[^1S_0]$. It should be noted that the contribution from $(c\bar{c})_{\mathbf{6}}[^1S_0]$ is zero if we take $h_1 = 0$ as indicated in Eq.(4).

In Fig.3 we plot the p_t -distributions and the y (rapidity)-distributions, where contributions

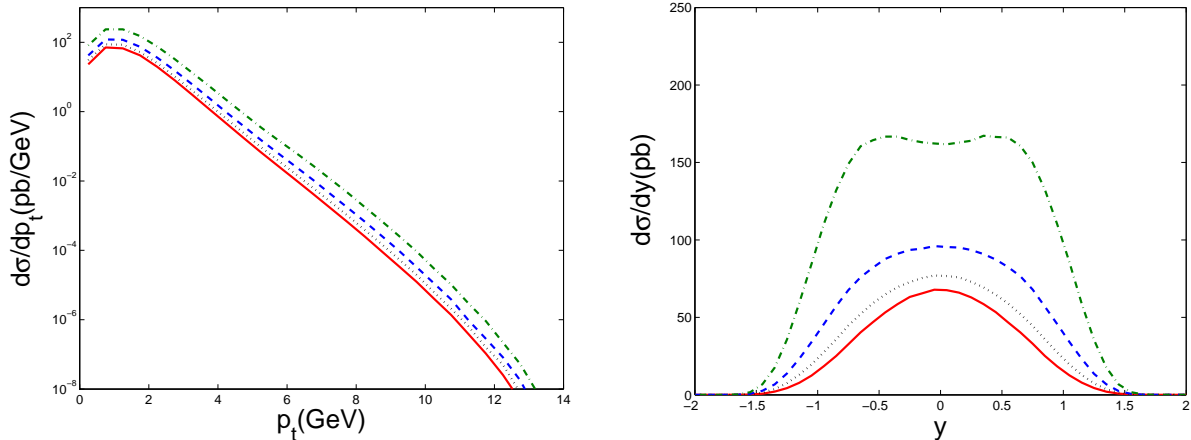


FIG. 3: The p_t -distributions (left) and y -distributions (right) for the hadroproduction of Ξ_{cc} at SELEX with different values of A_{in} . The dotted, the dashed and the dash-dot lines are for $A_{in} = 0.1\%$, 0.3% and 1% respectively. The result with CTEQ6HQ, i.e., $A_{in} = 0$ is shown by a solid line (the lowest one).

TABLE III: The R values for SELEX with the cut $p_t > 0.2$ GeV.

-	CTEQ6HQ($A_{in} = 0$)	$A_{in} = 0.1\%$	$A_{in} = 0.3\%$	$A_{in} = 1\%$
R	29.3	36.6	51.3	103.

from all the above mentioned sub-processes are summed up. Our results show that the p_t distributions do not change their shapes significantly, but the normalization changes. Also, as expected, the p_t differential cross-section becomes larger as A_{in} increases from 0 to 1%. The shapes of y -distributions and their normalization change significantly by changing A_{in} from 0 to 1%. With these results we may conclude that the intrinsic charm has significant impact on the production of Ξ_{cc} at SELEX.

Before the work of Ref.[25] and without taking the charm PDF into account, the Ξ_{cc} production at a hadron collider is believed to be through the sub-process $gg \rightarrow (cc)_{\bar{3}}[{}^3S_1]$. Now with the extrinsic/intrinsic charm and the $(cc)_{\mathbf{6}}[{}^1S_0]$ configuration contributions, there are additionally several other sub-processes which are non-negligible. To see how this alters the theoretical prediction based on the $gg \rightarrow (cc)_{\bar{3}}[{}^3S_1]$ subprocess, we introduce:

$$R = \frac{\sigma_{total}}{\sigma_{gg \rightarrow \Xi_{cc}((cc)_{\bar{3}}[{}^3S_1])}}, \quad (11)$$

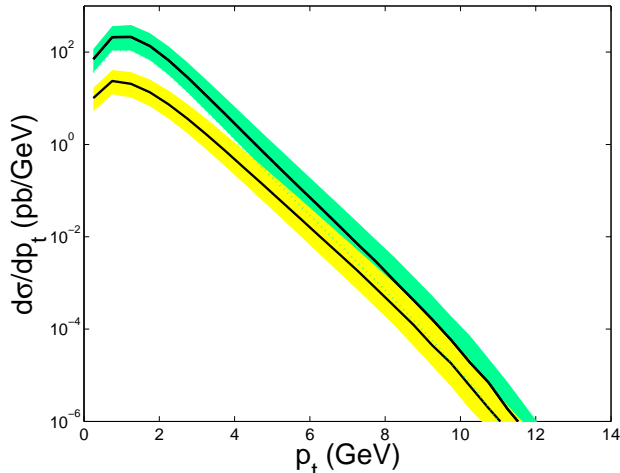


FIG. 4: The energy scale dependence of the p_t -distributions for $g + c$ mechanism at SELEX. The upper band is for the case of $(cc)_{\bar{3}}[{}^3S_1]$ and the lower band is for the case of $(cc)_{\bar{6}}[{}^1S_0]$, where the solid line in each band corresponds to $\mu = M_t$, the upper edge of the band is for $\mu = M_t/2$ and the lower edge is for $\mu = 2M_t$. Here the intrinsic charm has been taken into consideration, i.e. the PDFs of Eq.(6) with $A_{in} = 1\%$ are used.

where σ_{total} stands for the cross section with contributions from all sub-processes, including the intrinsic charm initiated ones; $\sigma_{gg \rightarrow \Xi_{cc}((cc)_{\bar{3}}[{}^3S_1])}$ is the cross section only from the subprocess $gg \rightarrow (cc)_{\bar{3}}[{}^3S_1]$. The numerical results of R for SELEX is given in TABLE.III. The results in TABLE.III show that the cross section at SELEX will be enhanced by including all the dominant sub-processes contributions. The enhancement can be even up to orders of magnitudes, e.g. the prediction for the production cross-section can be enhanced by order of about 10^2 for the case of $A_{in} = 1\%$. Hence it is possible to reduce the discrepancy between theory and experiment from the order of 10^3 to 10^1 .

Finally, we give some results of the uncertainty introduced by the factorization/renormalization scale. For clarity, we take the factorization scale μ_F and the renormalization scale μ_R to be the same, $\mu_F = \mu_R = \mu$, and take three typical choices for μ [31], i.e. $\mu = M_t$ (the default one in our calculations and $M_t \equiv \sqrt{M^2 + p_t^2}$), $\mu = 2M_t$ and $\mu = M_t/2$. The energy scale dependence of the p_t -distributions for $g + c$ mechanism are shown in FIG.4 for SELEX. Numerically, one may find that by taking $\mu = M_t/2$ (or $\mu = 2M_t$), the integrated cross-sections of the $g + c \rightarrow \Xi_{cc}$ mechanism (either for the $(cc)_{\bar{3}}[{}^3S_1]$ configuration or the $(cc)_{\bar{6}}[{}^1S_0]$ configuration) will be increased (or decreased) by about $(2.0 \sim 4.0)$ times

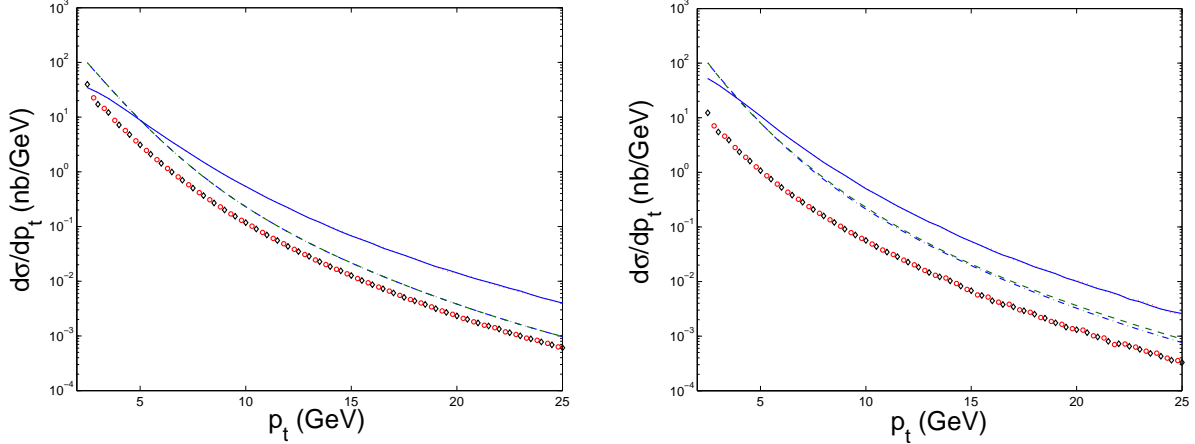


FIG. 5: The p_t -distributions for the hadroproduction of Ξ_{cc} at LHC. The left figure is for CMS or ATLAS with the rapidity cut $|y| \leq 1.5$ being adopted and the right one is for LHCb with the pseudo-rapidity cut $1.8 \leq |\eta| \leq 5.0$ being adopted. The solid line, the dash-dot line and the circle line correspond to that of the $g + g$, $g + c$ and $c + c$ mechanisms without the intrinsic charm being considered (the PDFs in CTEQ6HQ [8] are used) respectively. The dotted line, the dashed line and the diamond line correspond to that of the $g + g$, $g + c$ and $c + c$ mechanisms with the intrinsic charm being considered (the PDFs of Eq.(6) with $A_{in} = 1\%$ are used) respectively. The differences with and without intrinsic charm are so small, that, of them, only at LHCb for the $g + c$ mechanism the difference can be seen from the right figure.

to the case of $\mu = M_t$ within the allowable region of p_t .

B. Hadronic Production of Ξ_{cc} at Tevatron and LHC

We have evaluated the Ξ_{cc} production at ATLAS or CMS and LHCb at LHC (the center of mass energy $E_{cm} = 14$. TeV) and at CDF or D0 at TEVATRON (the center of mass energy $E_{cm} = 1.96$ TeV), where the intrinsic charm contribution is taken into account to see the possibility to observe the intrinsic charm effects at the high energy colliders. Since at LHC, the detectors ATLAS and CMS are similar, LHCb is quite different in rapidity cut; at TEVATRON the detectors CDF and D0 are similar, thus we will present the results bearing the similarity and difference in mind of the detectors. We plot the p_t -distributions in FIGs.(5,6) with or without the intrinsic of $A_{in} = 1\%$, where the used cuts in rapidity are also given and the PDFs is taken from CTEQ6HQ [8] directly. From the figures one

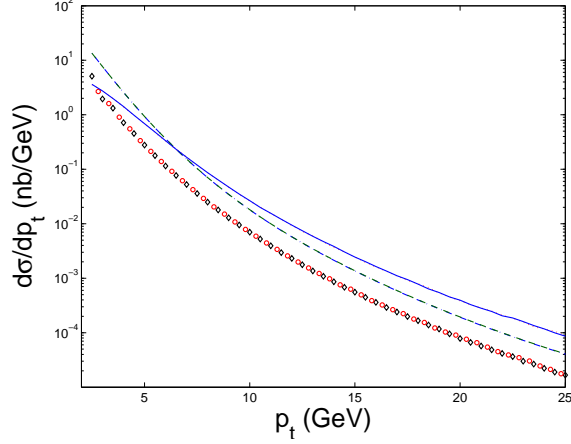


FIG. 6: The p_t -distributions for the hadroproduction of Ξ_{cc} at TEVATRON with the rapidity cut $|y| \leq 0.6$ being adopted. The meaning for the lines in the figure is the same as FIG.5. The differences between the two cases with and without intrinsic charm are too small to be seen.

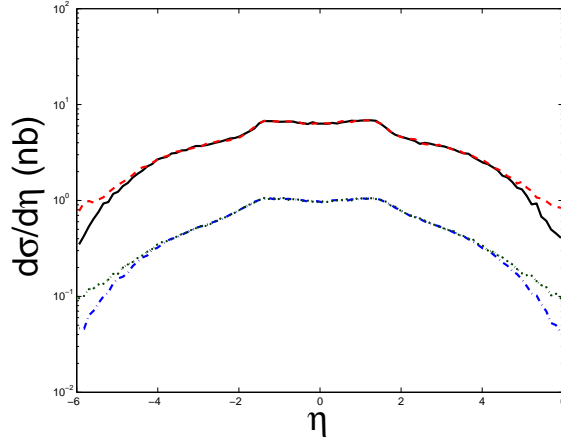


FIG. 7: The pseudo-rapidity η -distributions for the hadroproduction of Ξ_{cc} through the $g + c$ mechanism at LHC, where the p_t cut $p_t \geq 4$ GeV is adopted. The solid line, the dash-dot line correspond to the case of $(cc)_{\mathbf{\bar{3}}}[{}^3S_1]$ and the case of $(cc)_{\mathbf{6}}[{}^1S_0]$ without the intrinsic charm being considered (the PDFs in CTEQ6HQ [8] are used). The dashed line and the dotted line correspond to the case of $(cc)_{\mathbf{\bar{3}}}[{}^3S_1]$ and the case of $(cc)_{\mathbf{6}}[{}^1S_0]$ with the intrinsic charm being considered (the PDFs of Eq.(6) with $A_{in} = 1\%$ are used).

can see that for all of the mechanisms $g + g$, $g + c$ and $c + c$ at the detectors of LHC and TEVATRON, the differences in p_t -distributions for the two cases, i.e., with or without the intrinsic charm are too tiny to be seen in the most cases. The largest difference is found for

TABLE IV: Contributions from different sub processes to the cross sections for the hadronic production of Ξ_{cc} at Tevatron and LHC. The cut $p_t \geq 4$ GeV is taken for all the hadronic colliders. Additionally, the cut $|y| \leq 1.5$ is taken for LHC, the cut $1.8 \leq |\eta| \leq 5.0$ is taken at LHCb, and the cut $|y| \leq 0.6$ is taken at Tevatron.

-	Tevatron		LHC		LHCb	
-	$(cc)\bar{3}[^3S_1]$	$(cc)\mathbf{6}[^1S_0]$	$(cc)\bar{3}[^3S_1]$	$(cc)\mathbf{6}[^1S_0]$	$(cc)\bar{3}[^3S_1]$	$(cc)\mathbf{6}[^1S_0]$
σ_{gg} (nb)	1.61	0.399	22.3	5.44	25.7	6.47
σ_{gc} (nb)	2.31	0.361	22.1	3.42	20.6	3.00
σ_{cc} (nb)	0.755	0.0435	8.75	0.478	3.18	0.169

TABLE V: The value of ε as defined in Eq.(12) for the hadronic production of Ξ_{cc} at Tevatron and LHC. In the calculation, the cut $|y| \leq 1.5$ is taken for LHC, the cut $1.8 \leq |\eta| \leq 5.0$ is taken for LHCb, and the cut $|y| \leq 0.6$ is taken for Tevatron.

-	Tevatron			LHC			LHCb		
p_{tcut}	10 GeV	15 GeV	20 GeV	10 GeV	15 GeV	20 GeV	10 GeV	15 GeV	20 GeV
$\varepsilon_{gc}(p_{tcut})$	$\sim 1.1\%$	$\sim 1.2\%$	$\sim 2.2\%$	$\sim 0.1\%$	$\sim 0.2\%$	$\sim 0.5\%$	$\sim 6.1\%$	$\sim 10.0\%$	$\sim 15.0\%$
$\varepsilon_{cc}(p_{tcut})$	$\sim 1.5\%$	$\sim 2.2\%$	$\sim 4.3\%$	$\sim 0.4\%$	$\sim 0.5\%$	$\sim 0.6\%$	$\sim 0.8\%$	$\sim 2.0\%$	$\sim 3.5\%$

the mechanism $g+c$ at LHCb when p_t is larger than 15GeV (see the right figure in FIG.(5)). In order to see this more clearly, in Fig.(7), we plot the pseudo-rapidity distributions for the $g+c$ mechanism at LHC with a $p_{tcut} = 4$ GeV. It can be found that the difference for the two cases is sizable only at large pseudo-rapidity region.

In TABLE.IV we show the contributions from different sub-processes to the cross sections. Our results are given with cuts for different colliders and are derived by taking $A_{in} = 1\%$. From our results one can see that at Tevatron and LHC both $gg \rightarrow \Xi_{cc}$ subprocess and $gc \rightarrow \Xi_{cc}$ subprocess are dominant, unlike the situation at SELEX, where only the subprocess $gc \rightarrow \Xi_{cc}$ is dominant. This implies that the intrinsic charm has no significant impact on the Ξ_{cc} production at the Tevatron and LHC.

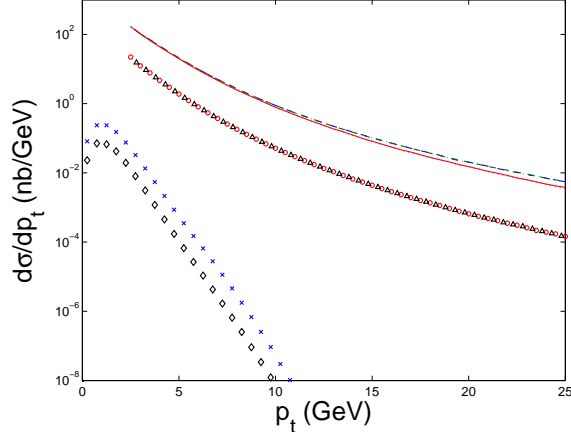


FIG. 8: The p_t -distributions for the hadroproduction of Ξ_{cc} . The dotted line, the dash-dot line, the circle line and the diamond line are those corresponding to LHCb, LHC, Tevatron and SELEX respectively with $A_{in} = 0$, respectively. The solid, the dashed line, the triangle line and the cross line are those corresponding to LHCb, LHC, Tevatron and SELEX with $A_{in} = 1\%$, respectively. Only at SELEX, the difference between the cases with and without intrinsic charm can be seen.

To see how intrinsic charm leads to different contributions in different p_t -regions, we introduce

$$\varepsilon_i(p_{tcut}) = \frac{\sigma_i(p_t \geq p_{tcut}) - \sigma_i^0(p_t \geq p_{tcut})}{\sigma_i^0(p_t \geq p_{tcut})} \times 100\%, \quad (12)$$

where $i = cc$ and $i = gc$ denote the contributions from the sub-processes $cc \rightarrow \Xi_{cc}$ and $gc \rightarrow \Xi_{cc}$, respectively. σ_i^0 denotes the cross section without the intrinsic charm, while σ denotes what with $A_{in} = 1\%$. The results for the ratio with different cuts are given in TABLE.V. From TABLE.V, one can see that by introducing intrinsic charm, the maximal change in the cross sections under various cuts is only about 10%. This leads us to conclude that it may be impossible to observe the effects of intrinsic charm at Tevatron and LHC through the Ξ_{cc} production.

Finally we give in Fig.8 the transverse distributions of Ξ_{cc} for different experiments. From Fig.8 we see that only at SELEX the effect of the intrinsic charm is significant because the sub-process $gc \rightarrow \Xi_{cc}$ is dominant one. At LHC and Tevatron, the sub-process $gg \rightarrow \Xi_{cc}$ becomes more important, and can even be dominant with the increasing p_t . This is the main reason why our results for LHC and Tevatron do not show any significant effect from the intrinsic charm.

IV. DISCUSSIONS AND SUMMARY

We have studied the Ξ_{cc} hadronic productions in experiments at SELEX, Tevatron and LHC. In our analysis we include contributions from various sub-processes, especially contributions from the intrinsic charm. For the intrinsic charm component inside a nucleon, we adopt the BHPS model [13]. Our results show that the intrinsic charm can have significant impact on the Ξ_{cc} production at SELEX. The cross section with certain reasonable kinematic cuts can be four times larger than that without considering the intrinsic charm. In contrast, the effect of the intrinsic charm is small at LHC and Tevatron. The main reason is that at those colliders with large energy, the contribution from the sub-process of gluon-gluon fusion becomes bigger than that from the sub-process of gluon-charm scattering (see TABLE.IV), and the intrinsic charm only makes a small effect on the gluon PDF (see Figs.1,2). Therefore, in comparison with all of the environments considered here and if the intrinsic charm component in a nucleon is really restricted in the region $A_{in} = 0.1\% - 1\%$ as for the BHPS model, then only at SELEX the Ξ_{cc} production is suitable for ‘measuring’ the intrinsic charm component inside the incident hadrons. This is one of our main results.

In the literature the hadronic production of Ξ_{cc} is believed to be dominated by the production of a cc pair through gluon-gluon fusion and the cc pair is in a $[^3S_1]_{\mathbf{3}}$ state, and it has been found that the predicted cross section based on this sub-process is much smaller than the experimental observation of SELEX, the discrepancy is roughly about 10^3 [3]. The transition probability of a cc pair in $[^1S_0]_{\mathbf{6}}$ configuration to Ξ_{cc} is of the same order in v as what the cc pair in $[^3S_1]_{\mathbf{3}}$ configuration [25], so that the extrinsic charm contribution can enhance the production cross section quite a lot[8]. Here we show that by taking all the contributions from the intrinsic charm into account, the prediction for the production cross-section can be enhanced by order of about 10^2 for the case of $A_{in} = 1\%$, the discrepancy hence is reduced. To obtain a final solution for the discrepancy a more detailed study is needed.

Acknowledgments: This work was supported in part by the Natural Science Foundation of China (NSFC). C.-F. Qiao was supported also in part by the Scientific Research Fund of GUCAS (NO. 055101BM03). X.-G. Wu thanks the support from the China Postdoctoral Science Foundation.

-
- [1] M. Mattson *et al.*, SELEX Collaboration, Phys. Rev. Lett. **89**, 112001(2002).
- [2] A. Ocherashvili *et al.*, SELEX Collaboration, Phys.Lett. **B628**, 18(2005).
- [3] V.V. Kiselev and A.K. Likhoded, hep-ph/0208231.
- [4] M. Moinester, Z.Phys. **A355**, 349(1996); V.V. Kiselev and A. Likhoded, hep-ph/0103169.
- [5] S.P. Baranov, Phys. Rev. **D54**, 3228(1996).
- [6] A.V. Berezhnoy, V.V. Kiselev, A.K. Likhoded and A.I. Onishchenko, Phys. Rev. **D57**, 4385(1998).
- [7] A.V. Berezhnoy, V.V. Kiselev and A.K. Likhoded, Phys.Atom.Nucl. **59**, 870(1996).
- [8] Chao-Hsi Chang, Cong-Feng Qiao, Jian-Xiong Wang and Xing-Gang Wu, Phys. Rev. **D73**, 094022(2006).
- [9] Jon Pumplin, Phys. Rev. **D73**, 114015(2006).
- [10] R. Vogt and S.J. Brodsky, Nucl. Phys. **B478**, 311(1996).
- [11] T. Gutierrez and R. Vogt, Nucl.Phys. **B539**, 189 (1999); G. Ingelman and M. Thunman, Z. Phys. **C73**, 505 (1997).
- [12] S. J. Brodsky, C. Peterson and N. Sakai, Phys. Rev. **D23**, 2745 (1981).
- [13] S.J. Brodsky, P. Hoyer, C. Peterson and N. Sakai, Phys.Lett. **B93**, 451(1980).
- [14] F.I. Olness, R.J. Scalise and W.K. Tung, Phys. Rev. **D59**, 014506(1998).
- [15] M.A.G. Aivazis, J.C. Collins, F.I. Olness and W.K. Tung, Phys. Rev. **D50**, 3102(1994); M.A.G. Aivazis, F. I. Olness and W.K. Tung, Phys. Rev. **D50**, 3085(1994).
- [16] J. Amundson, C. Schmidt, W.K. Tung and X.N. Wang, JHEP10, 031(2000).
- [17] S. J. Brodsky, B. Kopeliovich, I. Schmidt, J. Soffer, Phys. Rev. **D73**, 113005(2006).
- [18] S. Kretzer, H.L. Lai, F.I. Olness and W.K. Tung, Phys. Rev. **D69**, 114005(2004).
- [19] M. Glueck, E. Reya and A. Vogt, Eur.Phys.J. **C5**, 461(1998).
- [20] A.D. Martin, W.J. Stirling and R.S. Thorne, Phys.Lett. **B636**, 259(2006) and reference therein.
- [21] E. Hoffmann and R. Moore, Z.Phys. **C20**, 71(1983).
- [22] B. W. Harris, J. Smith and R. Vogt, Nucl.Phys. **B461**, 181(1996).
- [23] M. Franz, M. V. Polyakov and K. Goeke, Phys. Rev. **D62**, 074024 (2000).

- [24] G.T. Bodwin, E. Braaten and G. P. Lepage, Phys.Rev.D51 (1995) 1125,1995, Erratum-
ibid.D55 (1997) 5853.
- [25] J.P. Ma and Z.G. Si, Phys. Lett. **B568**, 135(2003).
- [26] V.A. Litvin and A.K. Likhoded, Phys.Atom.Nucl. **62**, 679(1999).
- [27] R.D. Field, *Applications of Perturbative QCD (Frontiers in Physics)*, published by Addison-
Wesley Publishing Company, Inc., Editer, David Pines, 1989.
- [28] Chao-Hsi Chang, Chafik Driouich, Paula Eerola and Xing-Gang Wu, Comput. Phys. Com-
mun. **159**, 192(2004); Chao-Hsi Chang, Jian-Xiong Wang and Xing-Gang Wu, Comput. Phys.
Commun. **174**, 241(2006); Chao-Hsi Chang, Jian-Xiong Wang and Xing-Gang Wu, Comput.
Phys. Commun. **175**, 624(2006). The package BCVEGPY itself is for hadronic production of
 B_c meson, but it can be changed for the case of Ξ_{cc} with small corrections.
- [29] Jian-Xiong Wang, Nucl. Instrum. Methods Phys. Res., Sect. A 534, 241 (2004).
- [30] Chao-Hsi Chang, Jian-Xiong Wang and Xing-Gang Wu, hep-ph/0702054.
- [31] M. Klasen, B.A. Kniehl, L.N. Mihaila and M. Steihauser, Phys. Rev. Lett. **89**, 032001 (2002);
Chao-Hsi Chang, Jian-Xiong Wang and Xing-Gang Wu, Phys. Rev. **D70**, 114019 (2004).